Application of Finite Volume Method for Structural Analysis

Saeed-Reza Sabbagh-Yazdi † and Milad Bayatlou ‡

†) Associate Professor, Civil Engineering Department of KNToosi University of Technology, SYazdi@kntu.ac.ir
‡) PostGraduate Student, Civil Engineering Departmen of KNToosi University of Technology, Bayatlou@gmail.com

No.1346, ValiAsr Street, 19697, Tehran, IRAN

Abstract: A two-dimensional unstructured Galerkin Finite Volume Method (GFVM) solver of structural problems is introduced and applied for a plane-strain case. The developed matrix free explicit solver computes stresses and displacements of 2D solid mechanic problems. The test case is a rectangular plate with a circular hole at the centre of it, under uniformly distributed loads on all its sides. The results of present iterative explicit solver are compared with the analytical solution of the very same case using the general thick-walled tube problem formulations. The performance of the introduced method is presented in terms of stress and strain contours, convergence diagrams and error charts.

Key-Words: *Constraint Free, Plane-Strain Problem, Internal Circular Hole, Galerkin Finite Volume Method, Analytical Solution, Distributed Load*.

1. INTRODUCTION

In recent decades and by the advances in micro processing technologies, reliability and applicability of numerical analysis has increased significantly. In this regard, Finite volume method (FVM) has earned a great reputation, especially in the field of computational fluid dynamic (CFD)(Zienkiewicz & Taylor, 1989), heat and mass transfer calculations(Bijelonja, Demirdžić, & Muzaferija, 2006). But nowadays, according to the high potentials of this method, chiefly in considering large displacements, researchers show interest in using FVM in solving computational solid mechanic (CSM) problems(Slone, Bailey, & Cross, 2003).

Prior to this, Finite Element Method (FEM) was the undisputed approach in field of CSM, especially with regard to deformation problems involving non-linear material analysis(Zienkiewicz & Taylor, 1989), but since FEM could face some difficulties such as volumetric locking in dealing with excessive displacements(Bijelonja, Demirdžić, & Muzaferija, 2006), the interest in using FVM as an alternative solution was increased.

FVM is developed from finite difference method (FDM) (Sabbagh-Yazdi, Mastorakis, & Esmaili, 2008) and unlike its predecessors which solve partial differential equation(s) on a set of grid points, integrates governing equation(s) over pre-defined sub-domains(Bijelonja, Demirdžić, & Muzaferija, 2006). So FVM, similar to FEM, have been developed for solution of mathematical models on unstructured meshes and By doing so, considering geometrical complexities of problem and the refinement of grid spacing in the regions with high gradient of dependent variables is possible.

2. GOVERNING EQUATIONS

The general mathematical model for continuum mechanics can be defined by Cauchy's equilibrium equations.

$$\rho\ddot{u} = S^T\sigma + b \tag{1}$$

Where ρ is the material density, $\ddot{u}$ is the acceleration, σ is the stress tensor and b is the body force.

For two dimensional problems and in x-y coordinate system, stress tensor would take the form of $\sigma_{xy} = [\sigma_x \quad \sigma_y \quad \tau_{xy}]^T$, acceleration is obtained from displacement vector $\vec{u} = [u_x \quad u_y]^T$ and operator S^T is defined as:

$$S^T = \begin{bmatrix} \frac{\partial}{\partial x} & 0 & \frac{\partial}{\partial y} \\ 0 & \frac{\partial}{\partial y} & \frac{\partial}{\partial x} \end{bmatrix} \quad (2)$$

So the matrix form of Cauchy's equilibrium equations in 2D x-y coordinate system is:

$$\rho \begin{Bmatrix} \frac{\partial^2 u_x}{\partial t^2} \\ \frac{\partial^2 u_y}{\partial t^2} \end{Bmatrix} = \begin{bmatrix} \frac{\partial}{\partial x} & 0 & \frac{\partial}{\partial y} \\ 0 & \frac{\partial}{\partial y} & \frac{\partial}{\partial x} \end{bmatrix} \begin{Bmatrix} \sigma_x \\ \sigma_y \\ \tau_{xy} \end{Bmatrix} + \begin{Bmatrix} b_x \\ b_y \end{Bmatrix} \quad (3)$$

For stress-strain relation, the common Hook equation can be used:

$$\sigma_{xy} = \boldsymbol{D}_{xy} \varepsilon_{xy} \quad (4)$$

Where $\varepsilon_{xy} = [\varepsilon_x \quad \varepsilon_y \quad \gamma_{xy}]^T$ is the strain tensor and $\boldsymbol{D}_{xy}$ is the 2D stiffness matrix which takes the following form:

$$\boldsymbol{D}_{xy} = \begin{bmatrix} D_{xy_{(1,1)}} & D_{xy_{(1,2)}} & D_{xy_{(1,3)}} \\ \vdots & D_{xy_{(2,2)}} & D_{xy_{(2,3)}} \\ Symmetry & \dots & D_{xy_{(3,3)}} \end{bmatrix} \quad (5)$$

So stress-strain relation is defined as:

$$\begin{aligned} \sigma_x &= D_{xy_{(1,1)}} \varepsilon_x + D_{xy_{(1,2)}} \varepsilon_y + D_{xy_{(1,3)}} \gamma_{xy} \\ \sigma_y &= D_{xy_{(1,2)}} \varepsilon_x + D_{xy_{(2,2)}} \varepsilon_y + D_{xy_{(2,3)}} \gamma_{xy} \\ \tau_{xy} &= D_{xy_{(1,3)}} \varepsilon_x + D_{xy_{(2,3)}} \varepsilon_y + D_{xy_{(3,3)}} \gamma_{xy} \end{aligned} \quad (6)$$

Considering the elastic behavior of material, the strains could be replaced by:

$$\varepsilon_x = \frac{\partial u_x}{\partial x} \quad \varepsilon_y = \frac{\partial u_y}{\partial y} \quad \gamma_{xy} = \frac{\partial u_x}{\partial y} + \frac{\partial u_y}{\partial x} \quad (7)$$

So the Cauchy's equilibrium equations in two Cartesian coordinate directions can be written as:

$$\begin{aligned} &\boldsymbol{\rho \frac{\partial^2 u_x}{\partial t^2}} \\ &= \frac{\partial}{\partial x} \overbrace{\left[C_1 \left(\frac{\partial u_x}{\partial x} \right) + C_2 \left(\frac{\partial u_y}{\partial y} \right) + C_3 \left(\frac{\partial u_x}{\partial y} + \frac{\partial u_y}{\partial x} \right) \right]}^{\sigma_x} \\ &+ \frac{\partial}{\partial y} \overbrace{\left[C_3 \left(\frac{\partial u_x}{\partial x} \right) + C_5 \left(\frac{\partial u_y}{\partial y} \right) + C_6 \left(\frac{\partial u_x}{\partial y} + \frac{\partial u_y}{\partial x} \right) \right]}^{\tau_{xy}} + b_x \\ &\boldsymbol{\rho \frac{\partial^2 u_y}{\partial t^2}} \\ &= \frac{\partial}{\partial y} \overbrace{\left[C_2 \left(\frac{\partial u_x}{\partial x} \right) + C_4 \left(\frac{\partial u_y}{\partial y} \right) + C_5 \left(\frac{\partial u_x}{\partial y} + \frac{\partial u_y}{\partial x} \right) \right]}^{\sigma_y} \\ &+ \frac{\partial}{\partial x} \overbrace{\left[C_3 \left(\frac{\partial u_x}{\partial x} \right) + C_5 \left(\frac{\partial u_y}{\partial y} \right) + C_6 \left(\frac{\partial u_x}{\partial y} + \frac{\partial u_y}{\partial x} \right) \right]}^{\tau_{xy}} + b_y \end{aligned} \quad (8)$$

Where coefficients C_1 *to* C_6 are:

$$\begin{aligned} C_1 &= D_{xy_{(1,1)}} \quad C_2 = D_{xy_{(1,2)}} \quad C_3 = D_{xy_{(1,3)}} \\ C_4 &= D_{xy_{(2,2)}} \quad C_5 = D_{xy_{(2,3)}} \quad C_6 = D_{xy_{(3,3)}} \end{aligned} \quad (9)$$

3. STIFFNES MATRIX

Contrary to typical 2D models, no simplifying assumptions were applied to the stiffness matrix and by doing so, it is possible to consider other aspects of material's behavior. Applying smeared crack approach, hardening and softening behavior in non-linear compression (He, Wu, Liew, & Wu, 2006) and anisotropy of materials are some examples of further developments which are conceivable by altering the entries of stiffness matrix.

One of the most common cases in 2D analysis of structures is Plane-Strain state, in which the material behaves Linear-Elastic and doesn't experience out of plane strains. In that case the stiffness matrix $\boldsymbol{D}_{xy}$ would be:

$$\boldsymbol{D}_{xy} = \begin{bmatrix} \frac{E(1-\upsilon)}{(1+\upsilon)(1-2\upsilon)} & \frac{E\upsilon}{(1+\upsilon)(1-2\upsilon)} & 0 \\ \vdots & \frac{E(1-\upsilon)}{(1+\upsilon)(1-2\upsilon)} & 0 \\ Symmetry & \dots & \frac{E}{2(1+\upsilon)} \end{bmatrix} \quad (10)$$

Based on equation (9), the coefficients C_1 *to* C_6 for plane-strain state are:

$$\begin{aligned} C_1 &= \frac{E(1-\upsilon)}{(1+\upsilon)(1-2\upsilon)} \quad C_2 = \frac{E\upsilon}{(1+\upsilon)(1-2\upsilon)} \\ C_3 &= 0 \quad C_4 = \frac{E(1-\upsilon)}{(1+\upsilon)(1-2\upsilon)} \\ C_5 &= 0 \quad C_6 = \frac{E}{2(1+\upsilon)} \end{aligned} \quad (11)$$

4. NUMERICAL MODEL

In order to discretize the Cauchy's equilibrium equations, the following form is considered:

$$\rho \frac{\partial^2 u_i}{\partial t^2} = \frac{\partial \sigma_{ij}}{\partial x_i} + b_i \quad ; j = 1, 2 \quad (12)$$

Where σ_{ij} is defined as:

$$\begin{aligned} \sigma_{11} &= C_1 \left(\frac{\partial u_x}{\partial x} \right) + C_2 \left(\frac{\partial u_y}{\partial y} \right) + C_3 \left(\frac{\partial u_x}{\partial y} + \frac{\partial u_y}{\partial x} \right) \\ \sigma_{12} &= C_3 \left(\frac{\partial u_x}{\partial x} \right) + C_5 \left(\frac{\partial u_y}{\partial y} \right) + C_6 \left(\frac{\partial u_x}{\partial y} + \frac{\partial u_y}{\partial x} \right) \end{aligned} \quad (13)$$

$$\sigma_{21} = C_3\left(\frac{\partial u_x}{\partial x}\right) + C_5\left(\frac{\partial u_y}{\partial y}\right) + C_6\left(\frac{\partial u_x}{\partial y} + \frac{\partial u_y}{\partial x}\right)$$

$$\sigma_{22} = C_2\left(\frac{\partial u_x}{\partial x}\right) + C_4\left(\frac{\partial u_y}{\partial y}\right) + C_5\left(\frac{\partial u_x}{\partial y} + \frac{\partial u_y}{\partial x}\right)$$

By introducing the stress vector $\vec{F_i} = \sigma_{i1}\hat{\imath} + \sigma_{i2}\hat{\jmath}$ the equation (12) could be rewritten as:

$$\rho\frac{\partial^2 u_i}{\partial t^2} = \vec{\nabla}\,\vec{F_i} + b_i \tag{14}$$

Then test function ω was multiplied with equation (14), and the result was integrated over sub-domain Ω.

$$\int_\Omega \omega\cdot\rho\frac{\partial^2 u_i}{\partial t^2}d\Omega = \int_\Omega \omega\cdot\left(\vec{\nabla}\cdot\vec{F_i}\right)d\Omega + \int_\Omega \omega\cdot b_i d\Omega \tag{15}$$

In the absence of body forces, the terms containing spatial derivatives can be integrated by part over the sub-domain Ω and then equation (15) may be written as:

$$\int_\Omega \omega\cdot\rho\frac{\partial^2 u_i}{\partial t^2}d\Omega = \left[\omega\cdot\vec{F_i}\right]_\Gamma - \int_\Omega\left(\vec{F_i}\cdot\vec{\nabla}\omega\right)d\Omega \tag{16}$$

According to Galerkin Method, the weighting function ω can be chosen equal to the interpolation function ϕ. For a triangular type element with three nodes, the linear interpolation function ϕ_k which is called shape function in FEM, takes the value of unity at desired node n, and zero at other neighboring nodes on opposite side k (Figure 2):

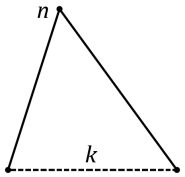

Figure (1): A linear triangular element.

Therefore the summation of the term $\left[\omega\cdot\vec{F_i}\right]_\Gamma$, which is calculated over the boundary of sub-domain Ω, equals zero. So the right hand side of equation (16) can be discretized as:

$$-\int_\Omega\left(\vec{F_i}\cdot\vec{\nabla}\omega\right)d\Omega = \frac{1}{2}\sum_{k=1}^{N}\left(\tilde{F_i}\cdot\overrightarrow{\Delta l}\right)_k \tag{17}$$

Where $\overrightarrow{\Delta l_k}$ is the normal vector of the side k and $\tilde{F_i}$ is the i direction piece wise constant stress vector at the centre of element associated with the boundary side k.

Since a linear triangular element forms the desired sub-domain, the left hand side of equation (16) can be discretized as:

$$\frac{\partial^2}{\partial t^2}\left(\int_\Omega \phi u_i d\Omega\right) \approx \frac{\Omega_\mathrm{n}}{3}\frac{d^2 u_i}{dt^2} \tag{18}$$

By applying the FDM concept in procedure of discretization, the time derivative of i direction displacement u_i in equation (18) can be described as:

$$\rho\frac{\Omega_\mathrm{n}}{3}\frac{d^2 u_i}{dt^2} = \rho\left(\frac{u_i^{t+\Delta t} - 2u_i^t + u_i^{t-\Delta t}}{(\Delta t)^2}\right)\frac{\Omega_\mathrm{n}}{3} \tag{19}$$

The term of body forces can also be written as:

$$\int_\Omega \omega\cdot b_i d\Omega = \frac{1}{3}b_i\Omega_\mathrm{n} \tag{20}$$

Eventually by using equations (17), (19) and (20), the Cauchy's equilibrium equations can be discretized as:

$$\left(\frac{u_i^{t+\Delta t} - 2u_i^t + u_i^{t-\Delta t}}{(\Delta t)^2}\right) = \frac{3}{2\rho\Omega_\mathrm{n}}\sum_{k=1}^{N}(\tilde{\sigma}_{i1}\Delta y - \tilde{\sigma}_{i2}\Delta x)_\mathrm{k} + \frac{b_i}{3\rho} \tag{21}$$

Considering direction $i = 1$ as x and $i = 2$ as y, the stresses $\tilde{\sigma}_{i1}$ and $\tilde{\sigma}_{i2}$ are computed as:

$$\begin{aligned}\sigma_{xx} &= C_1\frac{\partial u_x}{\partial x} + C_2\frac{\partial u_y}{\partial y} + C_3\left(\frac{\partial u_x}{\partial y} + \frac{\partial u_y}{\partial x}\right)\\ \sigma_{xy} = \sigma_{yx} &= C_3\frac{\partial u_x}{\partial x} + C_5\frac{\partial u_y}{\partial y} + C_6\left(\frac{\partial u_x}{\partial y} + \frac{\partial u_y}{\partial x}\right)\\ \sigma_{22} &= C_2\frac{\partial u_x}{\partial x} + C_4\frac{\partial u_y}{\partial y} + C_5\left(\frac{\partial u_x}{\partial y} + \frac{\partial u_y}{\partial x}\right)\end{aligned} \tag{22}$$

And finally:

$$\begin{aligned}\sigma_{xx} &= = \frac{1}{A_k}\sum_{m=1}^{N}\left(C_1 u_x\Delta y - C_2 u_y\Delta x + C_3\left(u_x\Delta y - u_y\Delta x\right)\right)_\mathrm{k}\\ \sigma_{xy} = \sigma_{yx} &= \frac{1}{A_k}\sum_{m=1}^{N}\left(C_3 u_x\Delta y - C_5 u_y\Delta x + C_6\left(u_x\Delta y - u_y\Delta x\right)\right)_\mathrm{k}\\ \sigma_{22} &= \frac{1}{A_k}\sum_{m=1}^{N}\left(C_2 u_x\Delta y - C_4 u_y\Delta x + C_5\left(u_x\Delta y - u_y\Delta x\right)\right)_\mathrm{k}\end{aligned} \tag{23}$$

where A_k is the area of triangular element associated with boundary side k of the sub-domain Ω_n (Figure (2):

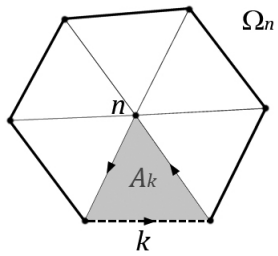

Figure (2): Triangular element with area A_k within the sub-domain Ω_n.

5. COMPUTATIONAL STEPPING

It is necessary to select proper time step limit in order to ensure that the stability of explicit solution is provided. Doing so, the time step for each control volume can be computed as:

$$\Delta t_n \leq \frac{r_n}{\mathbb{C}} \tag{24}$$

Where $\mathbb{C}$ is wave velocity and r_n is the average radius of equivalent circle that matches with the desired control volume. These parameters can be described as:

$$\mathbb{C} = \sqrt{\frac{E}{\rho(1-\upsilon^2)}} \tag{25}$$

$$r_n \leq \frac{\Omega_n}{P_n} \tag{26}$$

Where $P_n = \sum_{k=1}^{N_{Edge}} (\Delta l)_k$ is the perimeter of the 2D control volume.

Since the use of local time stepping greatly enhances the convergence rate, the local time step of each control volume is used for computation of static problems, so the computation of each control volume can advance using a pseudo time step which is calculated for its own control volume.

6. LOAD IMPOSING TECHNIQUE

In order to impose plane distributed loads on the boundaries, the contribution of distributed load q associated with the desired boundary node is replaced by an equivalent concentrated load P. The value of the concentrated load P_n at desired boundary node n is computed using the half the lengths of two boundary edges adjacent to that node;

$$P = \frac{q}{2}\sum_{k=1}^{2}(\Delta l)_k \tag{27}$$

In which $(\Delta l)_k = \sqrt{(\Delta x)_k^2 + (\Delta y)_k^2}$.

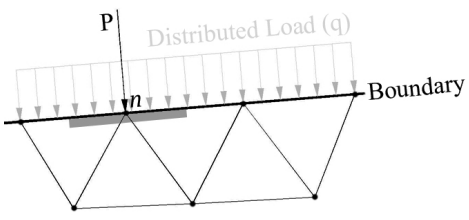

Figure (3): Equivalent concentrated load P associate with in plane distributed load q.

Since abrupt imposition of external loads can lead to instability of numerical solution, a gradual load imposing technique which uses a relaxation coefficient $0 < C_{Relax} \leq 1$ during some computational iterations is implemented in the present model.

$$C_{Relax} = Min\left\{\left(\frac{I_{Step}}{L/\Delta t}\right), 1.0\right\} \tag{28}$$

where I_{Step} is the iteration number at the desired stage of the computation and L is a length scale that can be assumed as the distance between maximum displacement and the centre of external load or constraint (support location).

7. COMPUTATIONAL RESULTS

In order to verify the accuracy of Galerkin Finite Volume Method (GFVM) solver, stress-strain analysis of a rectangular plate with a circular hole at its center under distributed load on all its sides is considered. The results of GFVM solver then compared to analytical solution which can be generated from the general thick-walled tube problem (Sadd, 2009).

The analytical solution of this particular case was obtained by assuming that the radius of the circular hole compared to the plate's dimensions is noticeably small. Consequently the stresses compared to redial distance from the center of circular hole can be described as:

$$\begin{aligned} \sigma_r &= T\left(1 - \frac{r_1^2}{r^2}\right) \\ \sigma_\theta &= T\left(1 + \frac{r_1^2}{r^2}\right) \end{aligned} \tag{29}$$

Where σ_r and σ_θ are radial and hoop stress respectively, T is the distributed load and r_1 is the radius of circular hole.

A schematic illustration of the test case setup is shown in figure (4) and plate specifications are described in table (1).

Table (1): Plate specifications

Plate specification	Value
Young's modulus (E)	$10'000 \;\; Pa$
Poisson's ratio (υ)	0.3
Density (ρ)	$0.0026 \;\; \frac{kg}{cm^3}$

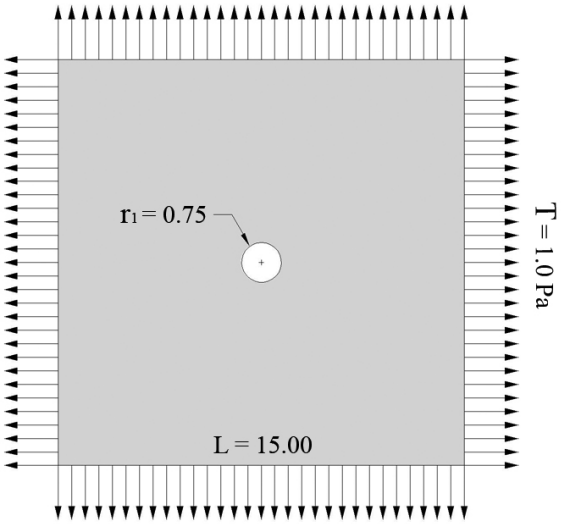

Figure (5): Schematic illustration of a plate with distributed loads on its boundaries.

In order to investigate the effects of mesh resolution on the accuracy of the results of present GFVM solver, computational results on two different meshes are compared.

Figure (7) shows two unstructured meshes which are used for the computing the stresses. Figure (8) and Figure (9) present the color coded maps of stresses which are computed by GFVM (using the Length Scale of 15m).

The convergence behavior of fine mesh's maximum displacement in terms of logarithmic root mean square is illustrated in Figure (6). As can be seen the numerical errors oscillate between 10^{-9} and $10^{-8.5}$.

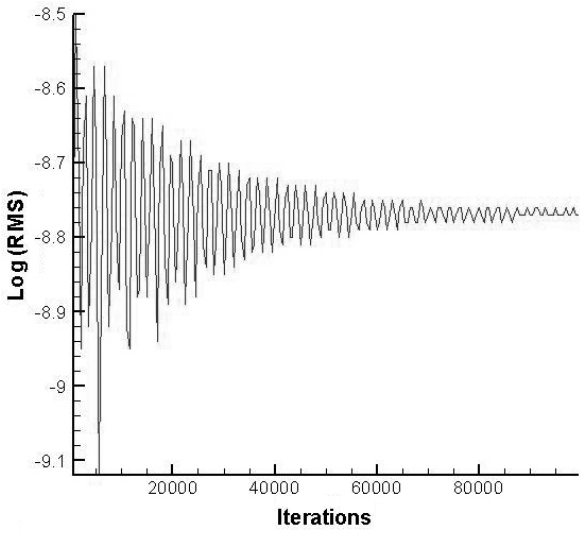

Figure (6): Convergence behavior in terms of logarithm of root mean squares for the mesh.

The accuracy of the results is assessed by comparing them with analytical answers. To do so, the evolvement of principal stresses in a horizontal section crossing the centre of circular hole is studied in Figure (10). The errors created by the variation of mentioned results are calculated for each individual node shown in Figure (11).

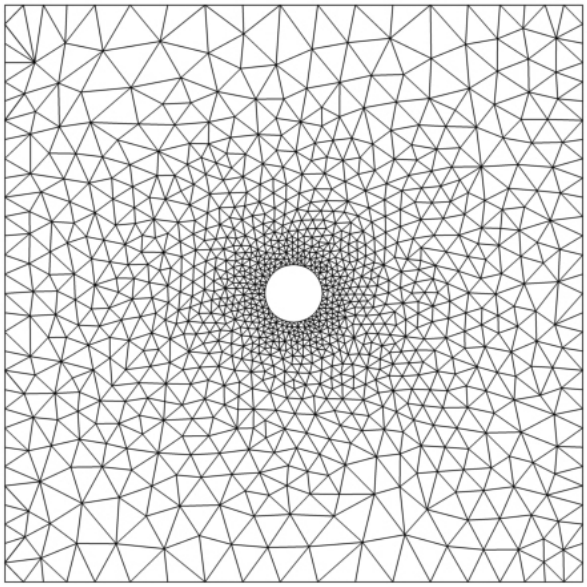

a) Coarse mesh.

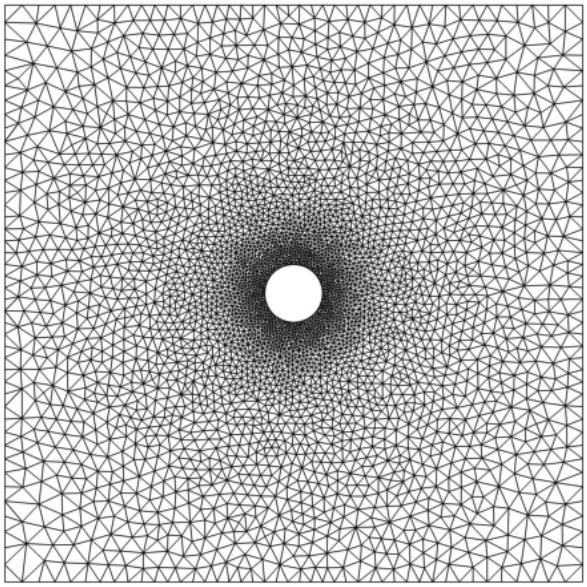

b) Fine mesh.

Figure (7): Unstructured meshes applied for the computations.

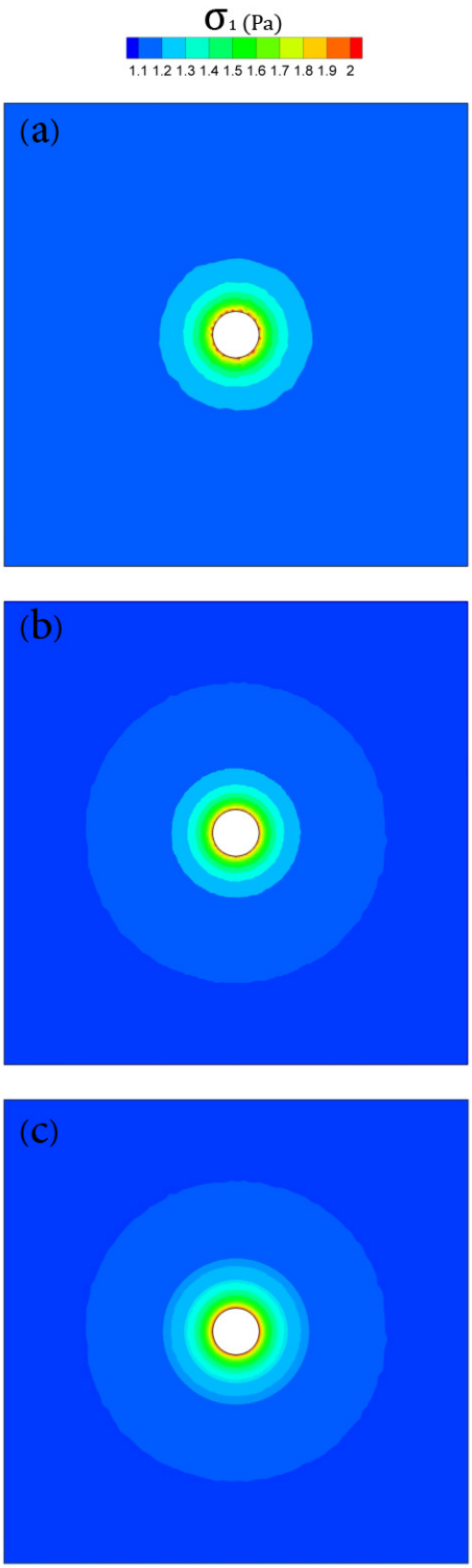

Figure (8): Color coded maps of computed 1st principal stress; **a)** Coarse mesh, **b)** Fine Mesh and **c)** Analytical Solution.

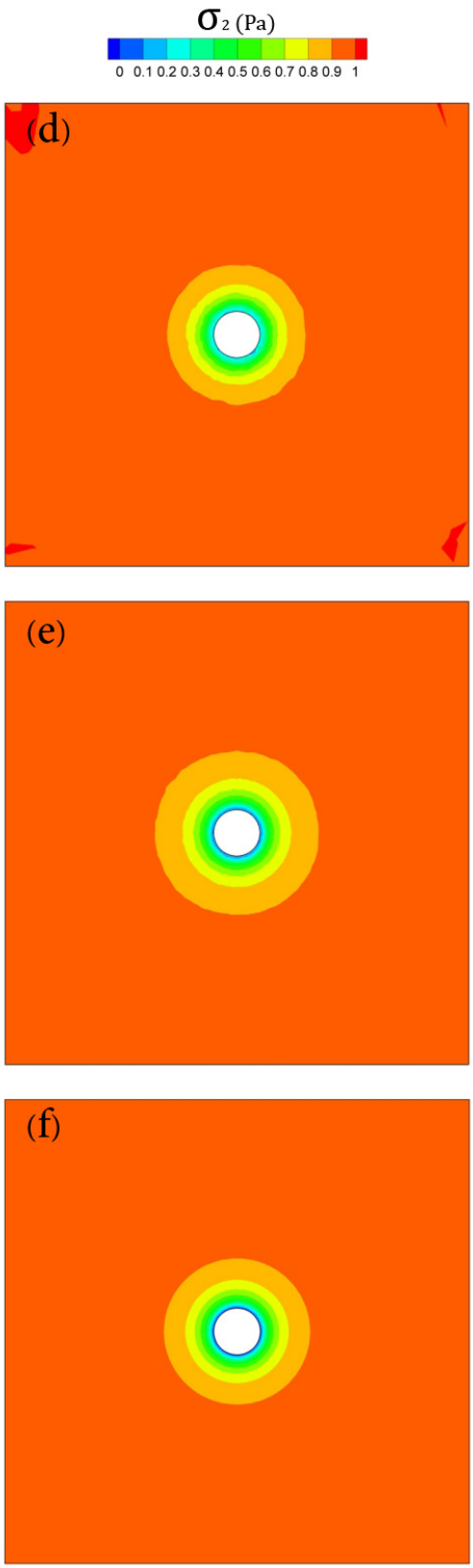

Figure (9): Color coded maps of computed 2nd principal stress; **d)** Coarse mesh, **e)** Fine Mesh an d **f)** Analytical Solution.

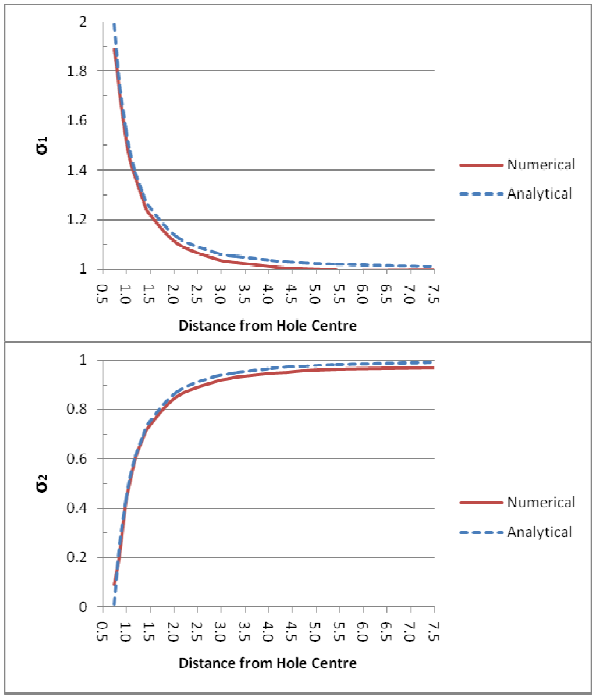

Figure (10): Comparison of principal stresses obtained from numerical and analytical methods.

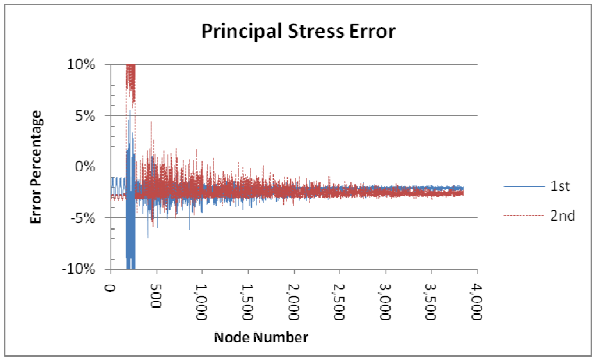

Figure (11): Error analysis of principal stresses.

8. Conclusion

In this paper, the vertex base Galerkin Finite Volume Method for explicit solution of the two dimensional Cauchy equilibrium equations is introduced and examined for a constraint free plane-strain rectangular plate with a circular hole in its centre under uniformly distributed loads on all sides. This computational model is designed to solve the solid mechanic problems on linear triangular unstructured triangular meshes and by establishing a general stiffness matrix, the possibility of further developments is considered.

The GFVM solver is verified by solving principal stresses for a benchmark plane-strain case under distributed loads. The performance of the computational solver is examined for various meshes with different mesh resolutions and the results were compared with the analytical solution results. The accuracy of the present GFVM model on relatively coarse mesh is in good agreements with the analytical solution results.

This shape function free computational model solves stress and deformation of solid mechanic problems under distributed loads without imposing any constraint. The fact that the solver produces accurate and stable results for the case without any constraint, proofs the robustness of the developed GFVM method.

So the new matrix free numerical method with light computational work load can easily be applied for solving real world solid mechanics problems.

9. Refrences

Bijelonja, I., Demirdz˘ic´, I., & Muzaferija, S. (2006). Finite Volume Method for Incompressible Linear Elasticity. *Journal of Mechanical Engineering* (195), 6378-639.

He, W., Wu, Y., Liew, K., & Wu, Z. (2006). A 2D total strain based constitutive model for predicting the behaviors of concrete structures. *International Journal of Engineering Science* (44), 1280–1303.

Sabbagh-Yazdi, S., Mastorakis, N., & Esmaili, M. (2008). Explicit 2D Matrix Free Galerkin Finite Volume Solution of Plane Strain Structural Problems on Triangular Meshes. *International Journal of Mathematics and Computers in Simulations* (2), 1-8.

Sadd, M. H. (2009). *Elasticity: Theory, Applications, and Numerics* (2nd Edition ed.). Oxford: Elsevier.

Slone, A., Bailey, C., & Cross, M. (2003). Dynamic Solid Mechanics Using Finite Volume Methods. *Applied Mathematical Modeling* (27), 69-87.

Zienkiewicz, O., & Taylor, R. (1989). *The Finite Element Method Basic Formulation and Linear Problems* (Vol. I). Maidenhead, UK: McGraw-Hill.